Chemical Science Review and Letters ISSN 2278-6783

www.chesci.com Research Article

Electroless Ni-Zn-P Ternary Deposits on Mild Steel with *Lawsone*

H. Asia Thabassoom* and J. Felicita Florence

Affiliated to Bharathidasan University, Tiruchirappalli-620020, India

Abstract

Electroless plating has gained popularity as a hard coating for industrial applications. The purpose of this work is to investigate the impact of *Lawsone*, which is extracted from *Lawsonia inermis Linn leaf extract*, on the electroless deposition of Ni-Zn-P alloys. Ni-Zn-P is analysed utilizing SEM, XRD, AFM, EDAX, and electrochemical techniques like potentiodynamic polarization curve and electrochemical impedance spectroscopy to determine its structure, morphologies, and corrosion resistance behaviour. The particular Ni-Zn-P alloy coating offers excellent mechanical properties as well as good corrosion resistance. The addition of *Lawsone* enhances the corrosion resistance property and the hardness of the deposits while modifying their structure and shape.

Keywords: *Lawsone, Lawsonia inermis Linn*, SEM, XRD, AFM, EDAX and Corrosion studies

***Correspondence**

Author: Asia Thabassoom.H

Email: thabassoomshahbir@gmail.com

Introduction

Chemical plating often called as Electroless deposition is a chemical manufacturing method used to deposit metal coatings on a range of substrates through the metal ion reduction chemically via autocatalysis in a liquid bath [10]. A conductive surface is plating, covered with a coating of metal [14]. Plating is used to beautify items for a variety of reasons, including preventing corrosion, increasing solder ability, decreasing friction, and enhancing paint adherence, change conductivity, and increase IR reflectance for radiation shielding [33, 24]. The oxidation reaction process, which lowers metal ions in an aqueous solution using a chemical reduction agent, provides the basis for the spin coating technique. There are numerous plating types and technologies [37, 22, 21, and 20].

Abner Brenner and Grace E. Riddell of the National Bureau of Standards discover the approach by incident that occurred in 1946 [10]. Little investigation has been conducted, according to the literature, on the electroless deposition of hydrated zinc crystallite under higher variable time effects. Due to the influence of zinc crystals and time-varying effects on the produced coating for advance application, this work aims to analyse the structural and corrosion properties of Ni-Zn-P coating. The introduction of zinc is as a result of it anti-corrosion ability [15, 23, 30, 39, 16]. Zinc is known to be more reactive than mild steel, thus will be able to attract almost all local oxidation and also improve mechanical properties of mild steel [28, 29,35, 26].

This plant used to treat hair is said to have antioxidant, anticarcinogenic, analgesic, antimitotic, immunomodulation, and nootropic effects. Mannitol, gallic acid, hennotannic acid, aliphatic components, triterpenes, sterols, phenolic derivatives, coumarins, xanthones, and other compounds that function as immune modulators and other supporting agents are just a few of the phytochemicals that are abundant in henna and have significant medical and pharmaceutical significance.

Lawsone has a melting point of 190°C and the chemical formula $C_{10}H_6O_3$. The trione system is only weakly stable; its three tautomer forms are 1, 2, 4-naphthotrione, 1, 2-naphthoquinone, and 1, 4 naphthoquinones. *Lawsonia inermis* exhibits remarkable properties that reduce rust [34,18,25]. *Lawsone* dye, derived from henna extract, is utilized in this work as an electroless complexing agent in the Ni-P bath. Its effective use as an additive and complexing agent in the enhanced electroless deposition of nickel P on mild steel will be straightforward and advantageous from a technological standpoint. Furthermore, it is quite sustainable.

Experimental Methods

Substrates consist of 12 cm by 6 cm by 0.5 mm mild steel samples. Each specimen has a hole drilled into one edge with a diameter of 2 mm for easy hanging in the solution during plating [3, 19, 1, and 12].

The nickel ion source, complexing agent, and reducing agent in the electroless bath are nickel sulphate (30 g/L), zinc sulphate (20 g/L), sodium hypophosphite (15 g/L), and sodium citrate (35 g/L), respectively. The pH of the bath is

changed using ammonium oxide. The autocatalytic reaction is kept at a temperature of 90°C, and the plating process takes 2.5 hours. The rate of deposition is determined by weight gain [4, 32, 17].

$$\text{Rate of depostion} = \frac{\text{Weight of the deposit} \times 10^4 \times 60}{\text{Area} \times \text{Density} \times \text{Time}} \quad (1)$$

Lawsone is isolated using Tommasi's method after being subjected to multiple stages of filtering, acidification, and diethyl ether extraction.

Table 1 Conditions and Composition of the Bath [12, 40, 6, and 7]

Bath constituents	Values	Operating conditions	Values
$NiSO_4.7H_2O$	20-35g/L	Temperature	(50-90)°C
$ZnSO_4.7H_2O$	15-20g/L	pH	(9-10)
$NaPO_2H_2{\cdot}H_2O$	10-20g/L	Duration of coating	2 and half hours
$Na_3C_6H_5O_7$	85g/L	Bath volume	500mL
NH_4Cl	50g/L		

Results and Discussion

Lawsonia inermis Linn Leaf qualitative estimation indicates the presence of the main component, *Lawsone*, and the principal coloring agent in significant amounts. This observation is consistent with earlier research such as Ni-P, Zn-P and Ni-W-P plating [34, 18].

UV Spectrum Analysis of Lawsone

Lawsone has a minor absorption band at 277 nm due to the presence of benzene and quinone with an electron-to-electron transition. The signal at 277 nm is caused by electrons moving sfrom the benzonoid ring to the quinonoid ring. The extended tail of the band at 334 nm in the visible area, which is due to the C=O and OH groups, is what gives *Lawsone* its yellow orange dye [25].

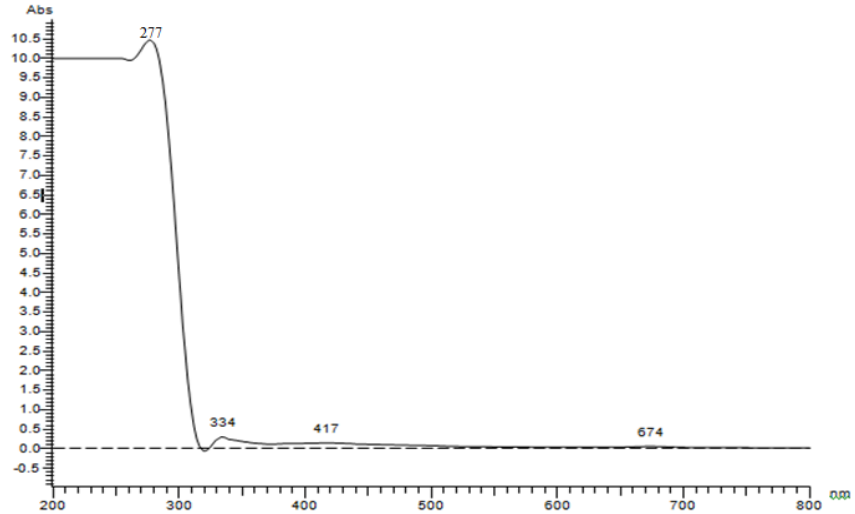

Figure 1 UV Spectrum [7]

FT-IR Spectrum Analysis of Lawsone

The stretching vibration of the hydroxyl group, which is present at the quinone ring of *Lawsone*, is responsible for the broadband in Figure with a centre at 3346 cm^{-1}. At 3346 cm^{-1}, the O-H stretching peak may be seen. 2974 cm-1 of the aromatic C-H stretching are visible [25].

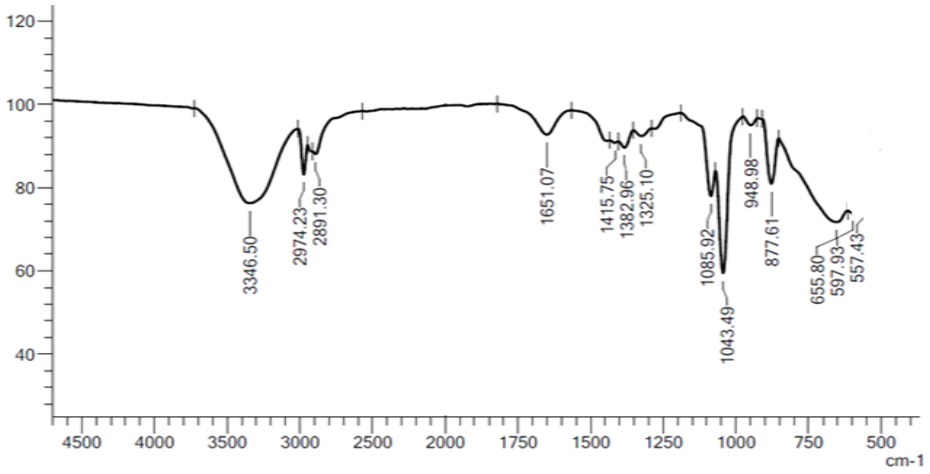

Figure 2 FTIR Spectrum [7]

Using sodium hypophosphite, zinc sulphate, sodium citrate, ammonium chloride, and *Lawsone* from *Lawsonia inermis Linn leaf* as reducing, complexing, accelerating, and adding agents, the current study aims to produce electroless Ni-Zn-P coated on mild steel [27,32, 40].

Effect of Lawsone

By adding 0.5–4mL of *Lawsone* to the basic bath composition for electroless Ni–Zn–P deposition, the effect of the addition agent is examined. The rate of deposition is higher when *Lawsone* is added at a 2mL dose. This demonstrates the impact of an addition agent on electroless deposition, which improves the pace of deposition and results in a brighter nickel deposit on mild steel. This is considered to be the ideal additive concentration.

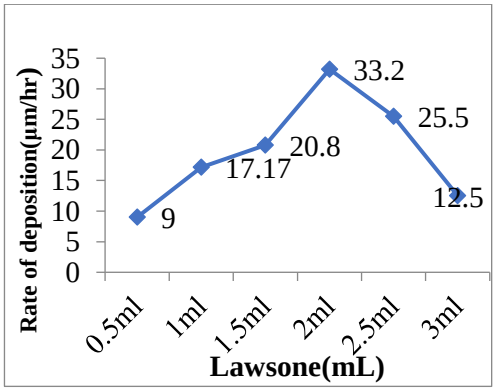

Figure 3 Effect of *Lawsone*

Table 2: Effect of *Lawsone*

Lawsone (mL)	Rate of deposition (µm/hr)
0.5ml	9.0
1ml	17.17
1.5ml	20.8
2ml	33.2
2.5ml	25.5
3ml	12.5
4ml	17.5

Effect of Nickel Sulphate

The Nickel sulphate hepta hydrate is a hydrate of Nickel sulphate containing nickel (in +2 oxidation state), sulphate and water moieties in the ratio 1:1:7. Ni content in the coatings increases as Ni ion concentration rises, activating the deposition process more quickly (with a lower Fe percentage). The concentration of nickel sulphate hepta hydrate has been varied from 10g/L to 40g/L by keeping the amount of addition agent *Lawsone* as 2mL, since the rate of deposition at 2ml is more. The greater deposition rate is obtained at a concentration of 30g/L. Therefore the optimum concentration of Nickel Sulphate hepta hydrate is 30g/L.

Effect of Sodium Hypophosphite

As the concentration of sodium hypophosphite monohydrate rises, so does the rate of deposition. For a sodium hypophosphite concentration of 15 g/L, the rate of deposition is 3.94 g/hr, which is greater than the rate for other sodium hypophosphite monohydrate concentrations. Therefore, it is thought that the optimal concentration is 15g/L.

Effect of Zinc Sulphate

The concentration of Zinc sulphate hepta hydrate has been varied from 5g/L to 30g/L by adding 5g/L at regular intervals, by keeping the amount of addition agent, *Lawsone* 2ml as constant. It is found that the greater deposition rate is obtained at a concentration of 20g/L. Therefore the optimum concentration of Nickel sulphate hepta hydrate is fixed as 20g/L [2].

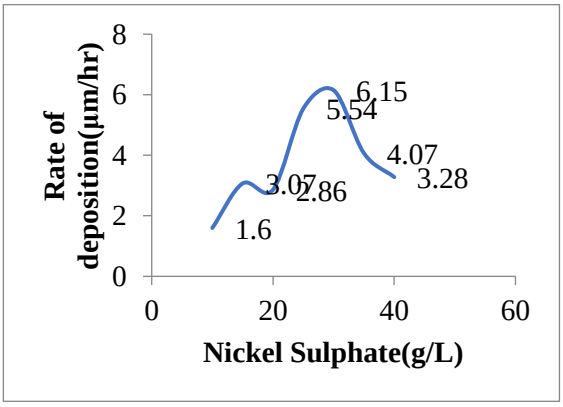

Table 3: $NiSO_4$

Nickel Sulphate (g/L)	Rate of deposition (µm/hr)
10	1.6
15	3.07
20	2.86
25	5.54
30	6.15
35	4.07
40	3.28

Figure 4 Effect of $NiSO_4$

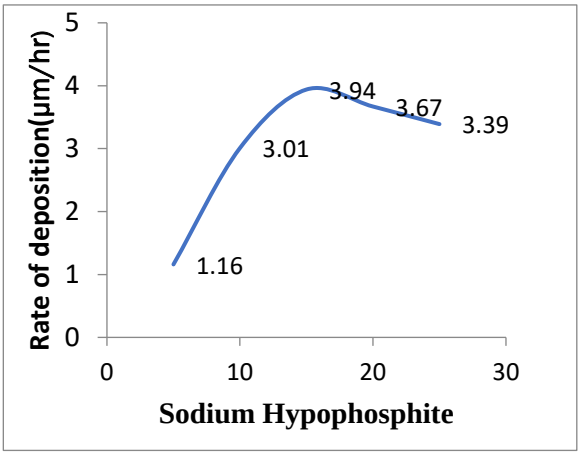

Table 4: Effect of Sodium Hypophosphite

Sodium hypophosphite monohydrate (g/L)	Rate of deposition (µm/hr)
5	1.16
10	3.01
15	3.94
20	3.67
25	3.39

Figure 5 Effect of Sodium Hypophosphite

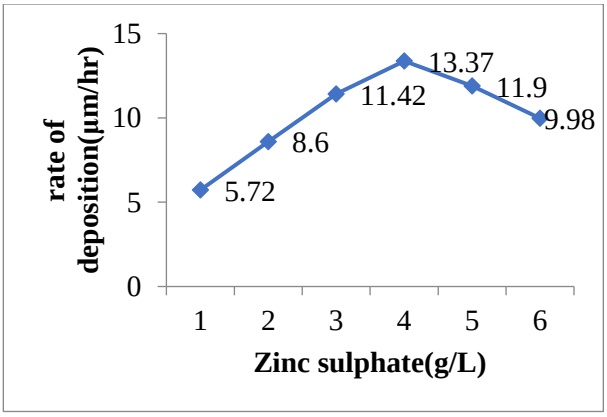

Table 5: Effect of Zinc Sulphate

Effect of Zinc sulphate (g/L)	Rate of Deposition (µm/hr)
5	5.72
10	8.6
15	11.42
20	13.37
25	11.9
30	9.98

Figure 6 Effect of Zinc Sulphate

Effect of Sodium Citrate

It is found from the table, by varying the concentration of Sodium Citrate Monohydrate the deposition rate is increased and it reaches the maximum at 50g/L. This is considered to be the ideal concentration for Ni-Zn-P electro less deposition when additive *Lawsone* is present.

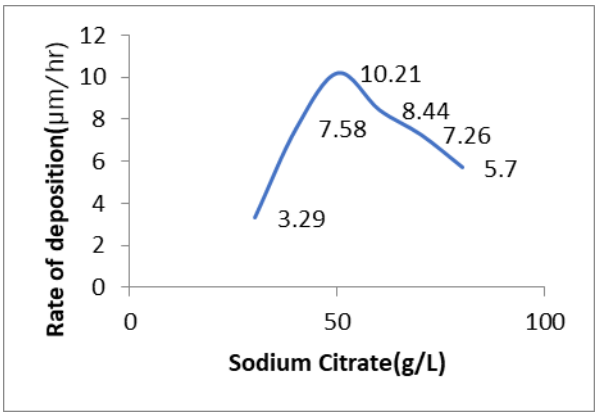

Table 6: Effect of Sodium Citrate

Effect of Sodium citrate (g/L)	Rate of Deposition (µm/hr)
30	3.29
40	7.58
50	10.21
60	8.44
70	7.26

Figure 7 Effect of Sodium Citrate

Effect of Ammonium Chloride

Ammonium chloride is used to regulate the pH of liquids. When the rate of deposition and ammonium chloride concentration both rise, which is found to be highest at 25g/L., therefore the bath containing 25g/L Ammonium Chloride is chosen as the optimum concentration for Ni-Zn-P electroless deposition.

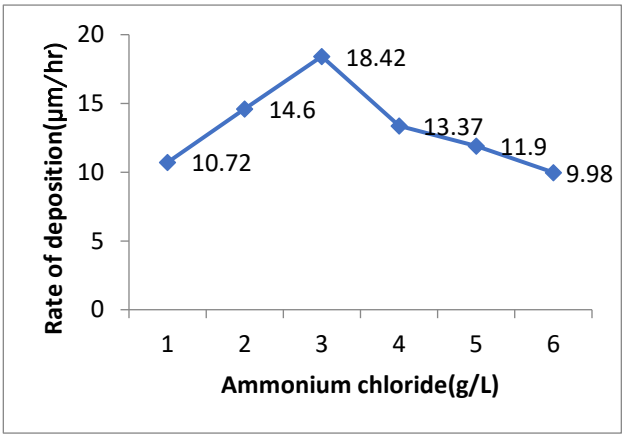

Table 7: Effect of Ammonium Chloride

Effect of Ammonium Chloride (g/L)	Rate of Deposition (µm/hr)
15	10.72
20	14.6
25	18.42
30	13.37
35	11.9
40	9.98

Figure 8 Effect of Ammonium Chloride

Effect of Temperature & pH

The temperature of the solution should also be closely monitored for consistent high quality deposits. The primary factor affecting the rate of the plating process is the temperature at which it takes place. The rate of plating rises exponentially with temperature. The weight of Ni-Zn-P deposition temperature rose from 50 to 90°C, as shown in Table. The rate of deposition dramatically increases as bath pH rises, and pH 9 is thought to be the ideal pH. The physical appearance at higher temperatures of 60-90°C is Bright. Because temperature creates the energy needed for the chemical bonding that results from metal oxidation, it has a major effect on the electroless bath. The table shows that the rate of deposition reaches a maximum at 90°C and a pH of 9, increasing with temperature and pH. [6]

Effect of Plating Time

According to table, the rate of deposition increases as plating time increases and is discovered to be greater at 150 minutes. This is considered to be the ideal plating period for *Lawsone*-assisted Ni-Zn-P electroless deposition.

Optimized Bath Composition

By modifying the different bath components in the presence of additive based on the rate of deposition, the bath composition can be selected for Ni-Zn-P electroless deposition in the presence of a Lawsone additive [12, 6, 38].

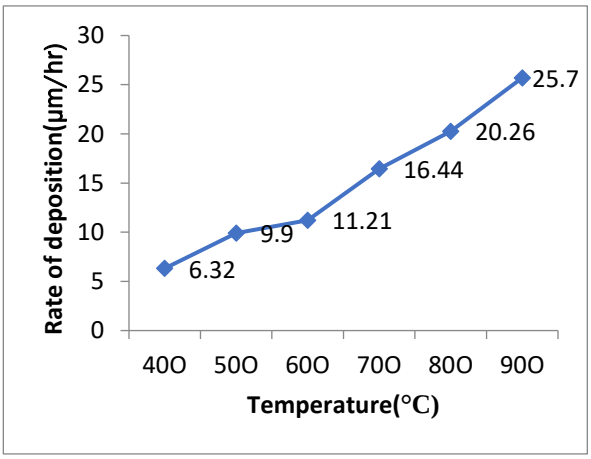

Table 8: Effect of Temperature and pH

Effect of Temperature (°C)	Rate of Deposition (µm/hr)
40^{O}	6.32
50^{O}	9.9
60^{O}	11.21
70^{O}	16.44
80^{O}	20.26
90^{O}	25.7

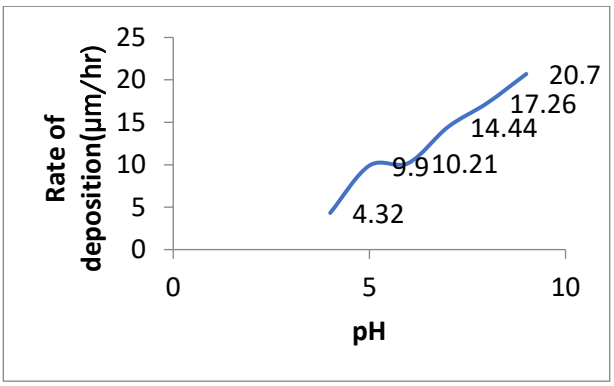

Table 8. Effect of temperature and pH

Effect of pH	Rate of Deposition (µm/hr)
4	4.32
5	9.9
6	10.21
7	14.44
8	17.26
9	20.7

Figure 9 Effect of Temperature and pH

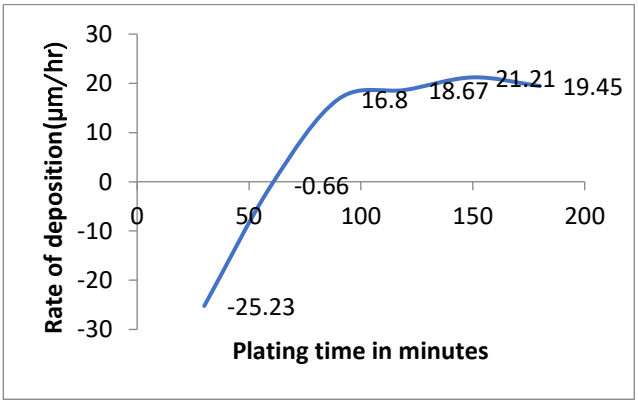

Table 9: Effect of Plating Time

Effect of Plating Time (g/L)	Rate of Deposition (µm/hr)
30	-25.23
60	-0.66
90	16.80
120	18.67
150	21.21
180	19.45

Figure 10 Effect of Plating Time

Nickel sulphate hepta hydrate	30g/L
Zinc Sulphate hepta hydrate	20g/L
Sodium hypophosphite	15g/L
Ammonium chloride	25g/L
Lawsone (2-Hydroxy-1,4-Napthoquinone)	2mL
pH	9
Temperature	90°C

Table 10: Optimized Bath Composition

Figure 11 Optimized Bath Composition

SEM Analysis on Metal Surface

SEM analyses provide a visible image of the metal surface. The surfaces of the electroless nickel-deposited mild steels BB and LA were evaluated using SEM examinations. The SEM pictures of the electroless nickel-deposited mild steels BB & LA are shown in **Figure 12** [(A), (B)]. For high Zn (II) ion concentration, SEM images of LA bath become smoother, more uniform, and some tiny holes appear. The amount of adsorbed Ni ions may decrease as a result of the rise in Zn (II) ion concentration because it may change how electro active species bind to substrate surfaces. As a result, there are fewer catalytic sites available and the rate of Ni deposition slows down. There are generally fewer nodules because BB slows down growth. *Lawsone*-produced deposits have consistent nodular formations, and the deposit characteristics are also good. Meanwhile, the results of the earlier study indicated that the Ni-W-P alloy should be deposited in order to produce the images of LA, which are uniform, compact, dazzling, and smooth with no visible defects such as peeling, pitting, cracking, bubbling, delamination, or nodulation [38].

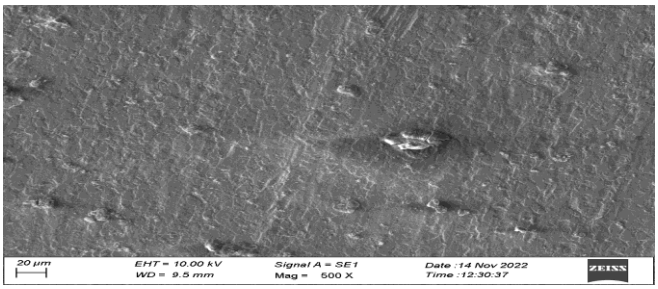

Figure 12 (A) SEM Photo Micrograph of Basic Bath.

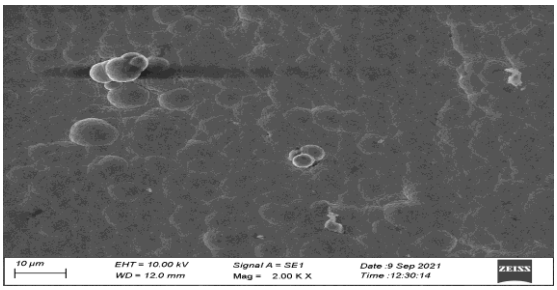

Figure 12 (B) SEM Photo Micrograph of LA Bath.

EDAX Analysis

Table 11, shows that the percentage of phosphorus varies from 5 to 15%, showing that the coating has a medium amount of phosphorous and is therefore quite hard. Nickel, zinc, and phosphorus elements are clearly present in the deposit, according to an investigation of EDAX. This bath's deposit has a globular morphology, good homogeneity, and a high deposition density. **Figure 13** [(A), (B)] displays the relative EDAX spectra of electroless Ni-Zn-P deposited on mild steel from BB and LA. The weight percentages of nickel, carbon, phosphorus, zinc, and oxygen in Ni-Zn-P electroless deposited mild steel from BB are found to be 73.26%, 3.58%, 13.36%, 6.69%, and 2.33%, respectively. It is found that the components that make up 75.31%, 3.09%, 11.92%, 5.69%, and 3.09% of the weight of LA are nickel, zinc, phosphorus, carbon, and oxygen, respectively. On adding additive the LA shows greater percentage compared to BB this is verified by above composition. The presence of *Lawsone* facilitates the more percentage of nickel and phosphorous to deposit on mild steel. The reduction in the percentage of carbon and oxygen reveals that the surface of deposits has no pores. Previous studies indicated that because the percentage of phosphorous in the coating varies from 2 to 12%, the Ni-W-P coating has a medium phosphorous concentration. It falls under the category of coatings with a high phosphorus content because of the significant amount of phosphorus. [13, 9]

Table 11, EDAX Analysis

Bath	Nickel (Wt %)	Zinc (Wt %)	Phosphorous (Wt %)	Carbon (Wt %)	Oxygen (Wt %)
BB	73.26	3.58	13.36	6.69	2.33
LA	75.31	3.09	11.92	5.69	3.09

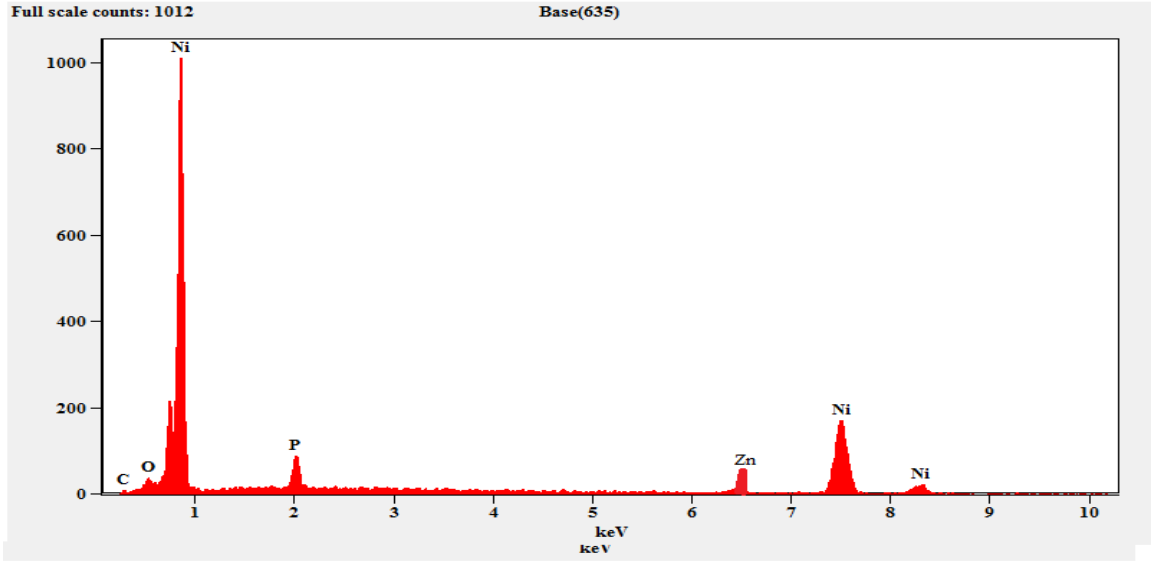

Figure 13 (A) EDAX Photograph Obtained of Basic Bath

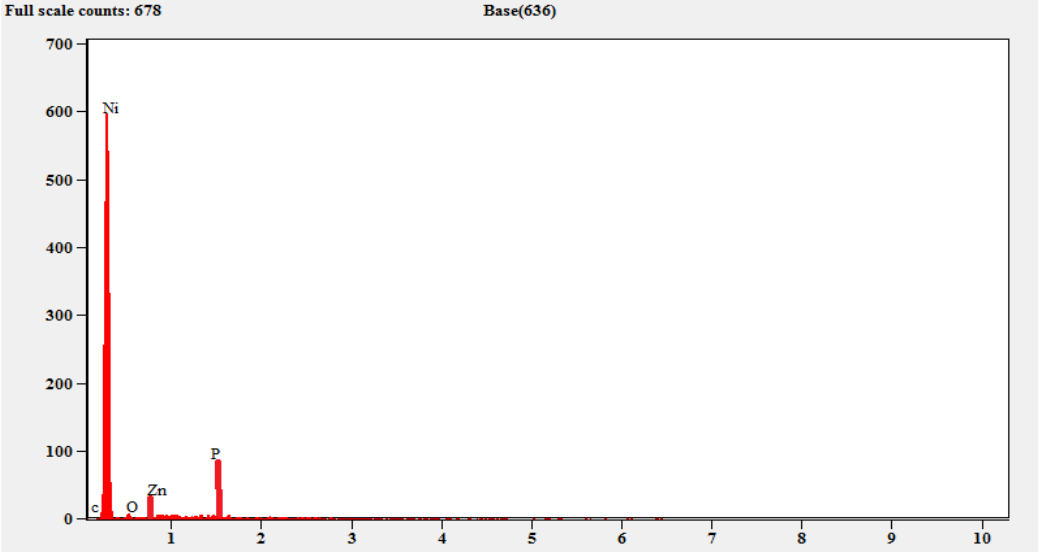

Figure 13 (B) EDAX Photograph Obtained of Bath

XRD Analysis

From several baths, an X-ray diffraction pattern of electroless Ni-Zn-P deposited on mild steel is obtained. Sharp peaks may be observed from BB at 29°, 45°, 52°, 65°, and 82°. The peak displays face-centered cubic structures as discrete (h k l) reflections. According to these findings, the mild steel substrate textures are grown parallel to the crystal planes shown in these patterns. The broad peak at 2 value of 40–50° in the XRD pattern indicates that the nickel–phosphorous alloys are amorphous in nature. For LA peaks arise at Ni (111) at 45°, P (200) at 52°, Zn (211) at 65°, P (200) at 76°and Ni (221) at 82° Bath deposits feature fine crystalline structures, although the degree of crystallographic deviation increases with thickness and time. The narrow peak is produced by the diffraction of the Nano crystalline phase in the electroless Ni-Zn-P deposit, and the sharp peak is produced by the (1 1 1) diffraction of Nano crystalline Ni. Beyond that, the amplitude of the previously deposited Ni-W-P coating showed an extreme rise, possibly indicating crystallization. Process variables including plating duration, pH level, bathing temperature, and complexing agents have an impact on the surface structure. For BB, LA the average computed crystal size is 62.22 nm, followed by 53.98 nm [8].

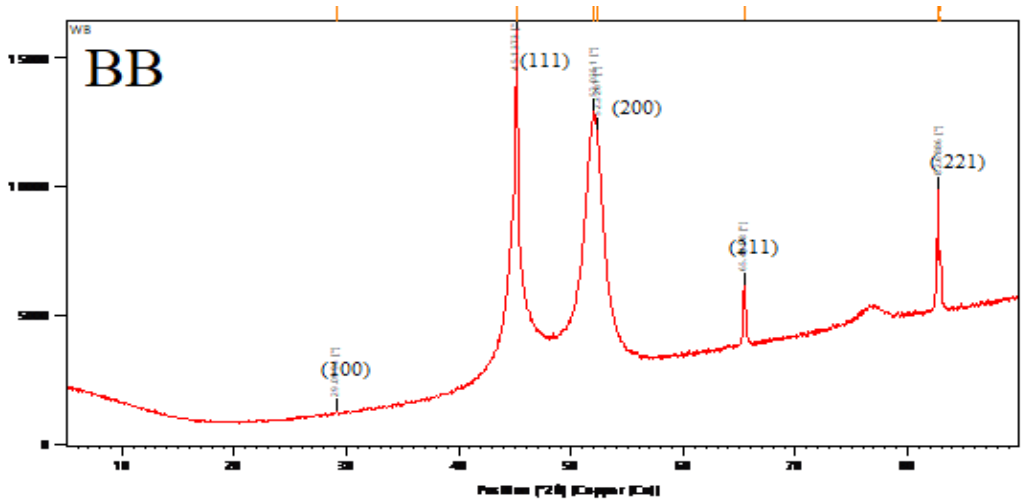

Figure 14 (A) XRD Photograph Obtained of Basic Bath

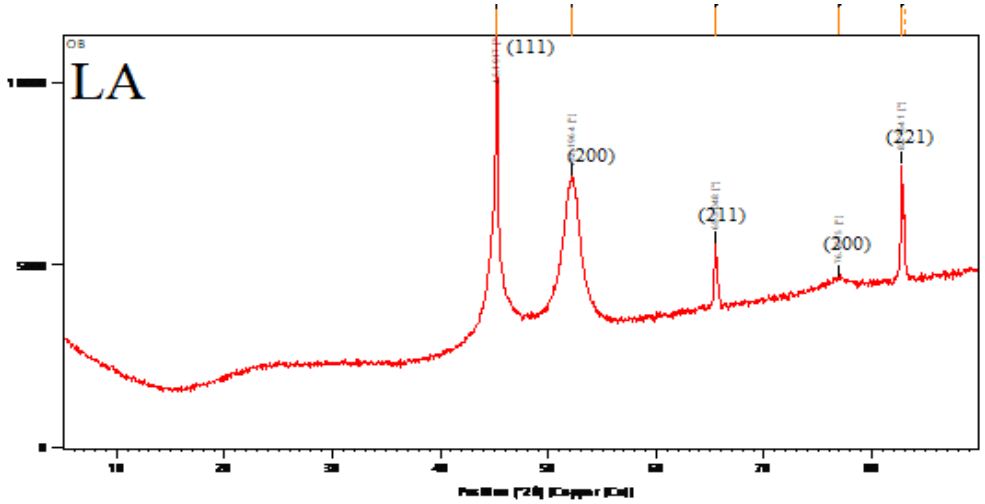

Figure 14 (B) XRD Photograph of LA Bath

Atomic Force Microscopy

Figure shows the AFM surface morphologies of the electroless Ni-P deposition on mild steel. The Ni-P deposits of the BB (in **Figure 14** (A)), LA (in Figure 14 (B)) are deposited at the ultrasonic power (100W). BB shows a rough surface with large nodules. LA shows rapid nuclei development, rapid nodule formation, and a significant number of tiny particles. The grain size is less than 100 nm. But in the presence of *Lawsone* as an addition agent crystal size becomes smaller. The crystal size of LA is smaller than 100 nm. According to AFM measurements, the electroless metal's average surface roughness (Ra) Ni-Zn-P deposited on mild steel for BB is 440.73 nm, LA is 249.54 nm.

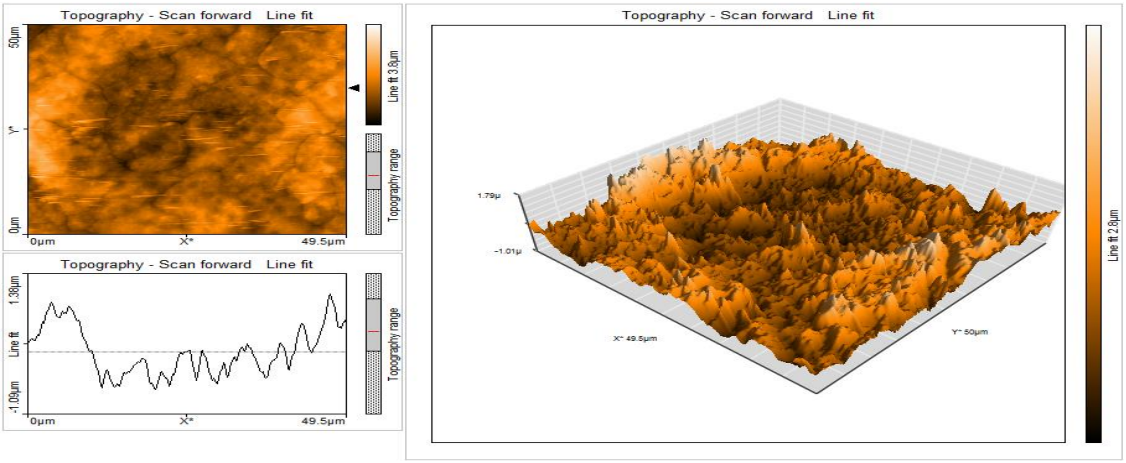

Figure 15 (A) AFM Photo Micrograph of Basic Bath

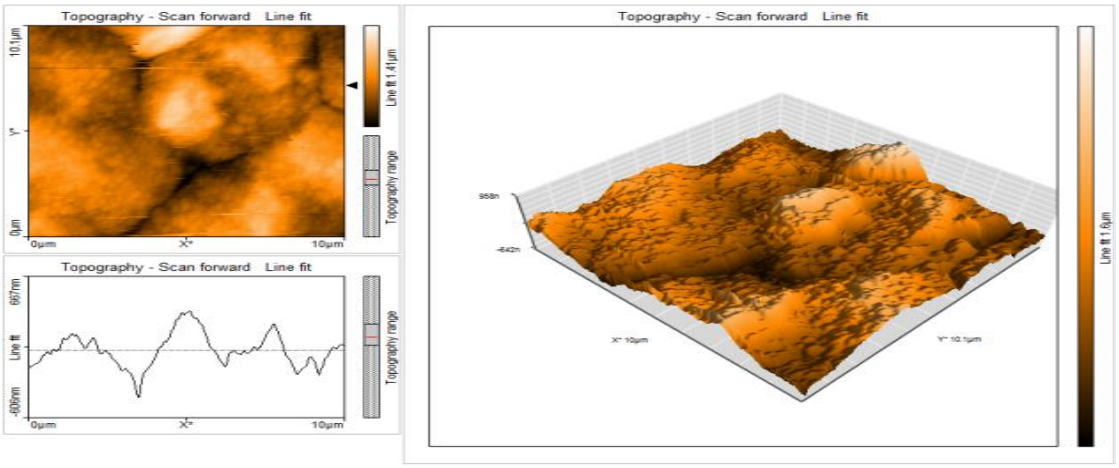

Figure 15 (B) AFM Photo Micrograph of LA Bath

Potentiodynamic Polarization Curves

Tafel curves of the Ni-Zn-P deposition on mild steel in 3.5 wt. % sodium chloride solutions are shown in **Figure 15**[(A), (B)]. In order to compare the corrosion current density, samples of an electroless bath of Ni-P-Zn deposited on mild steel surface are used. Table contains this information. According to Table, LA Bath exhibits greater corrosion resistance than BB (Constantine et al), [20] which is likely because the former coating contains a higher proportion of P in its composition. This coating offers better corrosion resistance than equivalent polycrystalline coatings because it is free from grain boundaries and has a passive glassy film on its surface. The structure of the coating changes from being crystalline to a mixture of amorphous and crystalline as the amount of P in the Ni-based electroless coating rises. The anodic curves are gradually shifting in the anodic direction, and it is found that the presence of *Lawsone* enhances the Ecorr and Icorr values in the Ni-P electroless deposited LA bath. The observations lead to the conclusion that a delayed correction will occur during the passivation of the mild steel that has been electroless deposited with LA-Zn-P in the presence of Lawsone. Out of all, LA has the smallest Icorr and the most noble Ecorr. Meanwhile, prior research indicated that the Ni-W-P deposition in 3.5% NaCl is comparatively resistant to corrosion. Phosphorus reduced the corrosion current density, which moved the corrosion potential to the right and demonstrated corrosion resistance [5].

Table 12 Tafel Polarization

Bath	E_{corr} (mV)	I_{corr} (µA)	R_{ct} (Ω cm^2)	Cdl (µF/Cm^2)
BB	-1 001.993 mV	549.661 µA	73	5.74×10^{-3}
LA	-996.422 mV	550.451 µA	20.82	6.24×10^{-4}

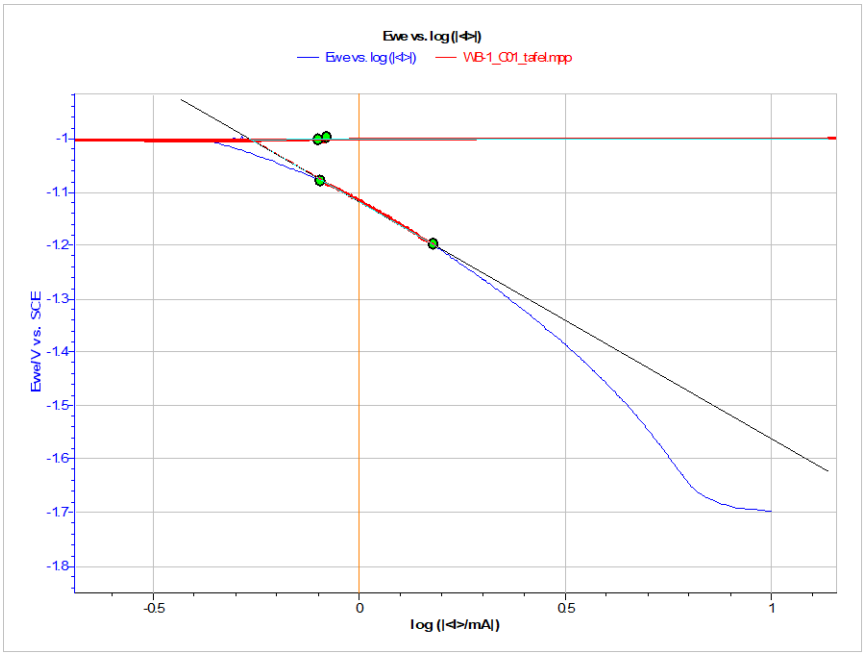

Figure 16 (A) Potentiodynamic Polarization Curve

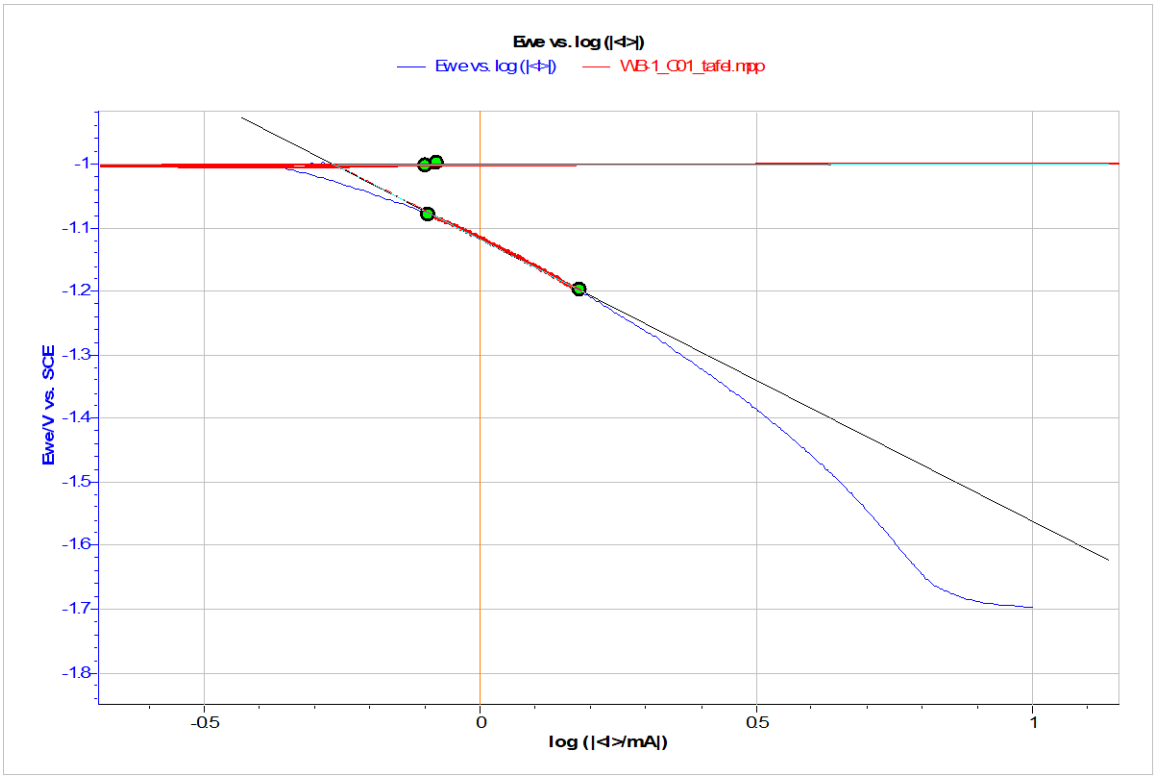

Figure 16 (B) Potentiodynamic Polarization Curve for LA Bath

Electrochemical Impedance Spectroscopy (EIS)

Figure 16 displays the Nyquist plot produced in a 3.5 weight percent NaCl solution at its different OCPs. It shows a semicircle followed by a rising trend, indicating the occurrence of a solid state diffusion process during the corrosion reaction. The EIS looks into the electroless Ni-Zn-P coating's capacity to resist corrosion on mild steel. NY Quist plots show that all curves have a single semicircle in the high frequency zone, which represents the charge-controlled reaction, and that all curves look similar. However, it should be highlighted that even if these curves seem to have the same shape, there are large differences in their sizes. The corrosion behavior of Ni-Zn-P coatings at their respective open circuit potentials in a 3.5% sodium chloride solution is shown in Figure [17]. Furthermore, the Ni-W-P indicated that inhibitor adsorption on the metal surface, solid surface inhomogeneity, and surface roughness are commonly cited as causes of the semicircle dip [38].

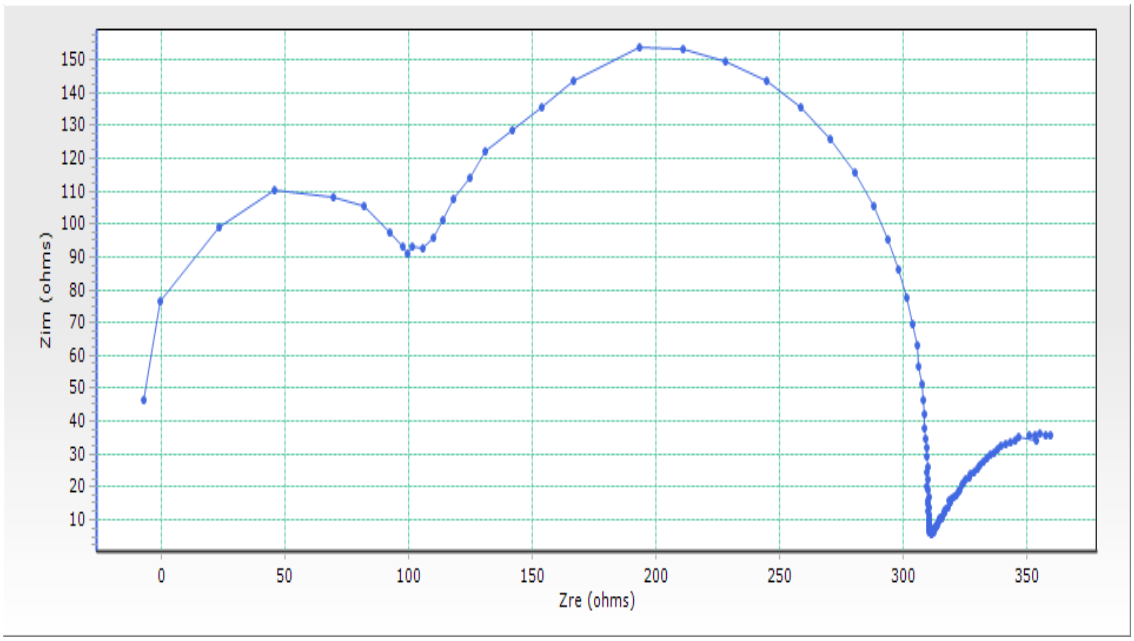

Figure 17 (A) AC Impedance Curve for Basic Bath

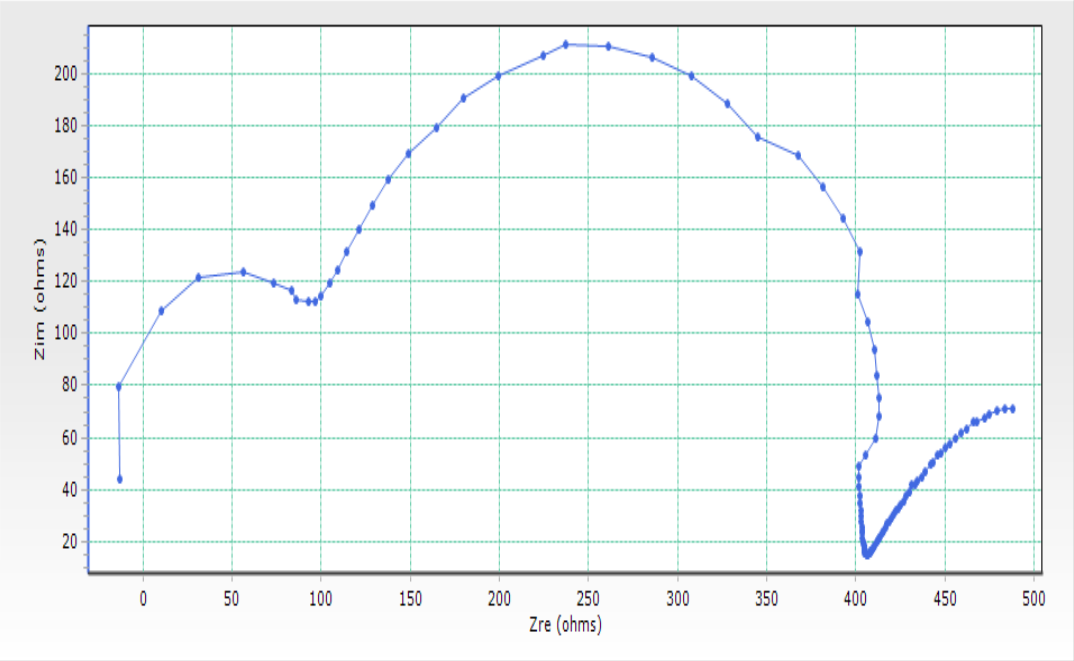

Figure 17 (B) AC Impedance Curve for LA Bath

Conclusion

This project successfully demonstrates the development of an innovative, biodegradable, and environmentally friendly electroless deposition technique using a Lawsone (LA) bath. The mild steel substrates were effectively coated with a Ni-Zn-P alloy, and the incorporation of Lawsone was confirmed through EDAX and FTIR analysis. The addition of *Lawsone* to the Ni-Zn-P alloy deposition process not only enhances the smoothness and uniformity of the coating but also improves its corrosion resistance. This indicates that the novel electroless deposition technique is both effective and environmentally friendly, aligning with the goals of using biodegradable materials and processes.

Acknowledgement

First, I thank you to Almighty for being able to complete this research work. I thank our institute Holy cross college and Jamal Mohamed College (Autonomous), Trichy for Lab facilities.

References:

[1] Ayoub.I.E, Ibrahim.I.B, and Dakroury.D.I, (2009), Surface Properties of Electroless Plated (Ni-P-Cu-W-Zn), J. Rad. Res. Appl. Sci., 2, 467-476.
[2] Asia Thabassoom.H and Felicita Florence.J, (2022), A study on the effect of Lawsone isolated from Lawsonia inermis Linn leaf extract Ni-W-P alloy electroless deposition, Research journal of chemistry and Environment, 26(9), 90-101.
[3] Amir Kordijazi, (2019), Optimization of Ni–P–Zn electroless bath and investigation of corrosion resistance of as-plated coatings, Materials Research Express, 6, DOI 10.1088/2053-1591/ab2a68.
[4] Asia Thabassoom and Felicita Florence.J, (2020), Electroless Nickel deposition on mild steel using Lawsone isolated from Lawsonia inermis Linn leaf, International journal of analytical and experimental modal analysis, XIII, 2107-2121.
[5] Asia Thabassoom.H, Femina.F, Felicita Florence.J, Kanmani.R and Amala Infant Joice.R, (2022), A Study on the Effect of Lawsone as Complexing Agent in the Electroless Zn-P Deposition, Oriental journal of chemistry, 38, 388-398.
[6] Available at https://byjus.com/jee/corrosion/
[7] Available from http://sigmaaldrich.com/
[8] Asia Thabassoom.H, Felicita Florence.J, (2022), Electroless Ni-W-P alloy deposition on Mild steel using Lawsone as Complexing agent, Oriental Journal of Chemistry, 38, 6, 1489-1497.
[9] Amir Ahmadi Ashitiani, Soheila Faraji, Sepideh Amjad Iranagh, Amir Hossein Faraji, (2017), The study of electroless Ni-P alloys with different complexing agents on CK45 steel substrate, Arabian journal of chemistry,

10, S1541-S1545. https://doi.org/10.1016/j.arabjc.2013.05.015
[10] Brenner. A, & Riddell.G.E. (1946), Electroless deposition of metal coatings, Journal of Research of the National Bureau of Standards, 36(3), 269-292. DOI: 10.6028/jres.036.027
[11] Balarajus.J.N, Rajam.K.S, (2005), Electroless deposition of Ni-Cu-P, Ni-W-P and Ni-W-Cu- P alloys., surface and coatings Technology, 195, 154-161.
[12] Di Bari.G.A, Alec Watson.S, (1983), A review of recent trends in nickel electroplating technology in North America and Europe, Metal Finishing Suppliers Association, 1-7.
[13] Fisher.R.D, Koopmans.D.E, (1964), Structure of electroless cobalt films, J. Electrochem Soc., 1964, 111, 264. DOI 10.1149/1.2426099
[14] Hsu.Y.H, & Duh.J.G, (2002), Electroless Ni-P and Ni-Zn-P coatings: Effect of zinc on the corrosion resistance & wear properties. Surface and Coatings Technology, 154(1), 118-123. DOI: 10.1016/S0257-8972(01)01197-7
[15] Ha.G.H, Kim.K.W, and Kim.J.K, (2004), "The effect of zinc content on the corrosion behavior of electroless Ni-Zn-P coatings." Journal of Electrochemical Society, 151(4), C227-C233. DOI: 10.1149/1.1645366.
[16] Hari Krishnan, John.S, Srinivasan.K.N, Praveen.J, Ganesan, (2006), An overall aspect of electroless Ni-P depositions—A review article, Metallurgical and Materials Transactions A., 37, 1917. https://doi.org/10.1007/s11661-006-0134-7
[17] Joseph Colaranotolo and Diane Tramontana, Electroless plating: fundamental and applications, American Electroplaters and Surface Finishers Society, Orlando, FL.1990, ISBN 9780936569079
[18] Khan.M.I, & Shah.A.A, (2016), Lawsone: A potential agent for electroless deposition. Journal of Applied Chemistry, 6(3), 145-151. DOI: 10.1080/0075865X.2016.1172345
[19] Karima Chouchane, Alexandra Levesque, Omar Aaboubi, Samuel Crequy, Nadir Mesrati and Jean Paul Chopart, (2015), Influence of zinc (II) ion concentration on Ni–Zn–P coatings deposited onto aluminium and their corrosion behavior, International Journal of Materials, Research. https://doi.org/10.3139/146.111155
[20] Kumar.K.S.S and Tiwari.K.K, (2009), "Effect of Zinc Content on the Properties of Electroless Ni-Zn-P Coatings." Materials Science and Engineering A, 510-511, 487-492. DOI: 10.1016/j.msea.2009.03.064.
[21] Koushik.A.P and Natarajan.S.K, (2005) "Electroless Ni-Zn-P coatings: Process optimization and properties." Surface and Coatings Technology, 200(3-4), 1291-1298. DOI: 10.1016/j.surfcoat.2005.02.015.
[22] Liang.B.T.C and Lin.C.C, (2010), "Corrosion resistance of electroless Ni-Zn-P coatings in various environments." Corrosion Science, 52(9), 2904-2911. DOI: 10.1016/j.corsci.2010.05.015.
[23] Lee.Y.H, Kim J.H, and Kim.M.H, "Study on the electroless Ni-Zn-P coatings and their properties for electronic applications." Journal of Materials Processing Technology, 2008, 201(1-3), 392-398. DOI: 10.1016/j.jmatprotec.2007.11.079.
[24] Morsy. M.A, & El-Hawary S.S, (2017), Phytochemical, antioxidant, and antibacterial activities of Lawsonia inermis L. (henna) extracts. Journal of Medicinal Plants Research, 11(20), 288-295. DOI: 10.5897/JMPR2017.6485
[25] Mehrdad Mahakam, Mehdi Nabati, Hadieh Rahbar Kafshboran., (2014), Isolation, identification and characterization of *Lawsone* from henna leaves powder with soxhlet technique, *Iranian Chemical Communication*, https://icc.journals.pnu.ac.ir
[26] Ojo Sunday Isaac Fayomi, Adedamola Sode, Godwin Akande, Oluranti Agboola,(2020), Improving the structural properties and corrosion behaviour of electroless deposited Ni-P-Zn coatings on mild steel for advanced processes, Research gate., DOI: 10.3934/matersci.2020.4.441
[27] Ostovari, Hoseineh.S.M., Peikari.M, (2009), Corrosion inhibition of mild steel in 1M HCl solution by henna extract: A comparative study of the inhibition by henna and its constituents (Lawsone, Gallic acid, α-D-Glucose and tannic acid, Corrosion science, 51, 1935-1949. https://doi.org/10.1016/j.corsci.2009.05.024
[28] Palaniappa, Veera Babu.G, Balasubramaniam.K, (2007), Electroless nickel–phosphorus plating on graphite powder, Materials Science and Engineering A, 47, 165-168. DOI: 10.1016/j.msea.2007.03.004
[29] Prasanta Sahoo, Suman Kalyan Das, (2019), Electroless Nickel – Phosphorous deposits, Book edition, 87-171. DOI: 10.1201/9780429466274-
[30] Ravi. M. R. K. S and Rao.K. K, (2018), "Recent advances in electroless Ni-Zn-P coatings: A review." Journal of Surface Engineered Materials and Advanced Technology, 2018, 8(1), 34-47. DOI: 10.4236/jsemat.2018.81004.
[31] Sappinandana Akamphona, Sittha Sukkasi, Yuttanant Boonyong maneerat, (2017), Reduction of Zinc consumption with enhances corrosion protection in hot-dip galvanized coatings: A process based on cost analysis, Resources, Conversation and Recycling, 58, 1-7.
[32] Sahib Mohammed Mahdi., (2017), Effect of henna (Lawsonia inermis) concentration on mild steel corrosion.

International Journal of Energy and Environment, 8, 321-330.
[33] Schmitz.J, & Reinders, (2000), Structural and corrosion properties of electroless Ni-P and Ni-Zn-P coatings. Journal of Electrochemical Society, 147(10), 3734-3741. DOI: 10.1149/1.1393491
[34] Singh.D, & Singh.H, (2015), Pharmacological properties of henna (Lawsonia inermis): A review. Journal of Pharmacognosy and Photochemistry, 4(4), 240-244.
[35] Seyyed Hashem Mousavi Anjidan, Masoud Sabzi, Mostafa Rohani Zadehb Mansour Farzam., (2018), the Effect of Electroless Bath Parameters and Heat Treatment on the Properties of Ni-P and Ni-P-Cu Composite Coatings, Materials Research, 21(2). https://doi.org/10.1590/1980-5373-MR-2017-0973
[36] Santhosh Yadav, Anil Kumar, Ashok Kumar., (2013), Essential perspective of Lawsonia inermis., International Journal of Pharmaceutical and Chemical Sciences., 2(2).
[37] Uddin. M.N, & Ghosh. A, (2014), Utilization of laws one as a complexing agent in electroless plating of nickel-phosphorus. Materials Science and Engineering B, 191, 35-42. DOI: 10.1016/j.mseb.2014.02.001
[38] Upadhyay.B, Dhaker.A.K, Singh.K.P, Kumar.A., A. Phytochemical analysis and influence of edaphic factors on Lawsone content of Lawsonia inermis L. Journal of Phyto. Res., 2010, 2(6), 47-54.
[39] Wang.X.Y, Xu.L.L, and Zhang.Z.Q, (2018), "Enhancing the performance of electroless Ni-Zn-P coatings with novel additives." Surface and Coatings Technology, 416, 127211. DOI: 10.1016/j.surfcoat.2021.127211.
[40] Wan Nik.W.B, Zulkifli.F, Rosliza.R. and Rahman. M.M, (2009), Lawsonia inermis as green inhibitor for corrosion protection of aluminium alloy, International Journal of Modern Engineering Research, 1, 723-728.

Publication History
Received 12.06.2024
Revised 21.09.2024
Accepted 22.09.2024
Online 30.09.2024